AUTOPHAGY
2019, VOL. 15, NO. 3, 478–492
https://doi.org/10.1080/15548627.2018.1522467

Taylor & Francis
Taylor & Francis Group

RESEARCH PAPER - BASIC SCIENCE

Mir223 restrains autophagy and promotes CNS inflammation by targeting ATG16L1

Yan Li[a], Dongmei Zhou[a], Yinghui Ren[b], Zimu Zhang[a], Xiangdong Guo[a], MingKun Ma[a,c], Zhenyi Xue[a], Jienv Lv[a,d], Hongkun Liu[a], Qing Xi[a], Long Jia[a], Lijuan Zhang[a], Ying Liu[a], Qi Zhang[e], Jun Yan[f], Yurong Da[a], Fei Gao[g], Jianbo Yue[h], Zhi Yao[a], and Rongxin Zhang[a,i]

[a]Laboratory of Immunology and Inflammation, Department of Immunology, Key Laboratory of Immune Microenvironment and Diseases of Educational Ministry of China, Tianjin Key Laboratory of Cellular and Molecular Immunology, Key Laboratory of Hormones and Development (Ministry of Health), Tianjin Medical University, Tianjin, China; [b]Tianjin Key Laboratory of Lung Cancer Metastasis and Tumor Microenvironment, Tianjin Lung Cancer Institute, Tianjin Medical University General Hospital, Tianjin, China; [c]Second Affiliated Hospital of Tianjin University of Traditional Chinese Medicine, Tianjin, China; [d]Hexi Women & Children Healthcare and Family Planning Service Center, Tianjin, China; [e]Institute of Integrative Medicines for Acute Abdominal Diseases, Nankai Hospital, Tianjin, China; [f]Tianjin Institute of Animal husbandry and veterinary, Tianjin, China; [g]State Key Laboratory of Reproductive Biology, Institute of Zoology, Chinese Academy of Sciences, Beijing, China; [h]Department of Biomedical Sciences, City University of Hong Kong, Hong Kong, China; [i]Guangdong Province Key Laboratory for Biotechnology Drug Candidates, School of Life Sciences and Biopharmaceutics, Guangdong Pharmaceutical University, Guangzhou, China

ABSTRACT

Microglia are innate immune cells in the central nervous system (CNS), that supplies neurons with key factors for executing autophagosomal/lysosomal functions. Macroautophagy/autophagy is a cellular catabolic process that maintains cell balance in response to stress-related stimulation. Abnormal autophagy occurs with many pathologies, such as cancer, and autoimmune and neurodegenerative diseases. Hence, clarification of the mechanisms of autophagy regulation is of utmost importance. Recently, researchers presented microRNAs (miRNAs) as novel and potent modulators of autophagic activity. Here, we found that *Mir223* deficiency significantly ameliorated CNS inflammation, demyelination and the clinical symptoms of experimental autoimmune encephalomyelitis (EAE) and increased resting microglia and autophagy in brain microglial cells. In contrast, the autophagy inhibitor 3-methylademine (3-MA) aggravated the clinical symptoms of EAE in wild-type (WT) and *Mir223*-deficienct mice. Furthermore, it was confirmed that *Mir223* deficiency in mice increased the protein expression of ATG16L1 (autophagy related 16-like 1 [S. cerevisiae]) and LC3-II in bone marrow-derived macrophage cells compared with cells from WT mice. Indeed, the cellular level of *Atg16l1* was decreased in BV2 cells upon *Mir223* overexpression and increased following the introduction of antagomirs. We also showed that the 3′ UTR of *Atg16l1* contained functional *Mir223*-responsive sequences and that overexpression of ATG16L1 returned autophagy to normal levels even in the presence of *Mir223* mimics. Collectively, these data indicate that *Mir223* is a novel and important regulator of autophagy and that *Atg16l1* is a *Mir223* target in this process, which may have implications for improving our understanding of the neuroinflammatory process of EAE.

Abbreviations: 3-MA: 3-methylademine; ACTB/β-actin: actin, beta; ATG: autophagy related; ATG16L1: autophagy related 16-like 1 (S. cerevisiae); BECN1: beclin 1, autophagy related; CNR2: cannabinoid receptor 2 (macrophage); CNS: central nervous system; CQ: chloroquine; EAE: experimental autoimmune encephalomyelitis; FOXO3: forkhead box O3; GAPDH: glyceraldehyde-3-phosphate dehydrogenase; H&E: hematoxylin and eosin; ITGAM: integrin alpha M; LPS: lipoplysaccharide; MAP1LC3/LC3: microtubule-associated protein 1 light chain 3; miRNAs: microRNAs; MS: multiple sclerosis; PPARG: peroxisome proliferator activated receptor gamma; PTPRC: protein tyrosine phosphatase, receptor type, C; RA: rheumatoid arthritis; SQSTM1: sequestosome 1; TB: tuberculosis; TIMM23: translocase of inner mitochondrial membrane 23; TLR: toll-like receptor.

ARTICLE HISTORY
Received 21 April 2017
Revised 22 August 2018
Accepted 4 September 2018

KEYWORDS
ATG16L1; autophagy; CNS inflammation; experimental autoimmune encephalomyelitis; microglia; *Mir223*

Introduction

EAE is the classical mouse model of human multiple sclerosis (MS), a chronic inflammatory disease that is characterized by demyelination and degeneration of axonal destruction in the CNS. Although the etiopathogenesis has not been well elucidated, a cascade of studies shows that EAE is trigged by the disruption of the blood-brain-barrier, as well as the activation of microglia and lymphocytes [1–4].

Microglia are the first line of defense in the CNS; they belong to the mononuclear phagocytic family and serve to clear pathogens in the initiation and sustenance of neuroinflammation. The functions of microglia in MS are complex and not well understood, though it has been well established

CONTACT Rongxin Zhang rxzhang@tmu.edu.cn; rongxinz@yahoo.com; Zhi Yao yaozhi@tmu.edu.cn Laboratory of Immunology and Inflammation, Department of Immunology, Key Laboratory of Immune Microenvironment and Diseases of Educational Ministry of China, Tianjin Key Laboratory of Cellular and Molecular Immunology, Key Laboratory of Hormones and Development (Ministry of Health), Tianjin Medical University, Tianjin 300070, China
Supplemental data for this article can be accessed here.

that microglia contribute significantly to the overall disease severity of MS. In fact, activated microglial nodules are the hallmark of MS lesion formation [5]. Overactive microglia are responsible for detrimental effects leading to profound neurological impairments [6], most of which occur by damage to the mitochondria.

It has been reported recently that enhancement of autophagy could ameliorate the pathogenesis of MS or EAE disease through the limitation of neuro-inflammation [7–9]. Neuro-inflammation and autophagy are 2 critical cellular processes that regulate each other to affect the progression of various diseases in the CNS. The relationship between these 2 processes is complex and includes the suppression of neuro-inflammation by autophagy. However, the signaling mechanisms that relieve this autophagy-mediated inhibition of inflammation to permit a beneficial inflammatory response remain unknown. Recent research found that regulating microglial activation by modulating mitophagy contributes to neuronal survival in Parkinson disease [10], and microglia autophagy plays an important role in the regulation of Parkinson disease [11]. In addition, inhibition of neuro-inflammation by autophagy has great benefits in ischemia [12].

Autophagy is a highly conserved catabolic pathway in the cell that degrades and recycles long-lived proteins and damaged organelles through lysosomal digestion [13]. Autophagy is active at a basal level under normal conditions, but it is rapidly upregulated following exposure to stress factors, including nutrient/hormone deprivation, hypoxic stress, accumulation of misfolded proteins and bacterial invasion [14,15]. Autophagy plays important roles in various organismal processes, such as development and aging, whereas abnormal autophagy leads to pathologies, including autoimmune and neurodegenerative diseases and cancer [16–19]. It has been reported that inducing autophagy could ameliorate several neurodegenerative diseases [20,21], and inhibit inflammation, especially in inflammatory or immune cells such as macrophages and dendritic cells [22,23].

Autophagy involves the formation of double-membrane vesicles in the cytosol called autophagosomes. These autophagosomes eventually fuse with lysosomes to form autolysosomes, where they are degraded and recycled [13,24]. However, the exact assembly platform and membrane source for the generation of these initial structures are still debated. The most likely organelles to provide membranes include specialized phosphatidylinositol-3-phosphate-enriched endoplasmic reticulum domains the Golgi apparatus. There are several important protein complexes that play a key role during autophagosome formation, including the ULK1 (unc-51 like kinase 1) complex, the class III phosphatidylinositol 3-kinase complex, ATG2-WIPI (WD repeat domain, phosphoinositide-interacting) protein complex, the ATG9 cycling system, and the ATG12–ATG5-ATG16L1 and MAP1LC3/LC3 (microtubule associated protein 1 light chain 3) or GABARAP conjugation systems [25]. Mitophagy, a classic type of cargo-specific autophagy, is the process of catabolism of mitochondria through their encapsulation by compartments termed phagophores (the precursors to autophagosomes) that are coated with the marker LC3 [26]. LC3 protein is covalently conjugated to the lipid phosphatidylethanolamine on the surface of phagophores [27]. LC3 must be cleaved by ATG4 proteins before conjugation with phosphatidylethanolamine [28,29]. While free LC3 (also called LC3-I) is soluble, its lipid-conjugated form (LC3-II) is associated with phagophores and complete autophagosomes. Hence, LC3 conjugation is used as a molecular marker of autophagosome generation and accumulation [30]. Chloroquine (CQ) is considered a lysosomotropic agent that can be trapped in lysosomes to inhibit lysosomal acidification and the activity of the degradative enzymes. Therefore, cells treated with CQ cannot undergo lysosomal digestion and exhibit autophagic vacuole accumulation [31].

The mechanisms regulating mammalian autophagy still require further investigation. Accumulating data have indicated that miRNAs play an important role in autophagy regulation [32,33]. miRNAs control biological events either by triggering the degradation of their target mRNAs through recognition of specific sequences, miRNA response elements (MREs), in the 3' UTR, and/or through inhibition of their translation. Recent reports have provided evidence that under stress conditions, a number of miRNAs, including *Mir144* [34], *Mir142, Mir106, Mir93*, and *Mir20*, are capable of modulating autophagy by changing the intracellular levels of key autophagy proteins. *Mir223* plays roles in monocytes/macrophages and embryonic stem cell differentiation, osteoclast formation, and bone remodeling. Microarray analyses of miRNA expression found that *Mir223* is enriched in microglia [35] and significantly upregulated in MS patients, and therefore the *MIR223* expression profile is a promising diagnostic biomarker for MS [36]. *mir223* knockout ($mir223^{-/-}$) mice develop less severe EAE, with increased myeloid-derived suppressor cell numbers in the spleen and spinal cord [37].

However, whether autophagy in microglia plays a role in the $mir223^{-/-}$ mediated alleviation of neuro-inflammation remains unclear. Here, we discovered that *Mir223* deficiency significantly ameliorated CNS inflammation, demyelination and the clinical symptoms of EAE and increased the number of resting microglia and the amount of autophagy in brain microglial cells. In contrast, the autophagy inhibitor 3-MA aggravated the clinical symptoms of EAE in WT and $mir223^{-/-}$ mice. Furthermore, we discovered that *Mir223* blocked starvation- and lipoplysaccharide (LPS)-induced autophagy in microglial BV2 cell lines. In light of our results, we provide evidence that a key autophagy protein, ATG16L1, is an important and direct autophagy-related target of *Mir223*.

Results

Mir223 *deficiency suppresses pathogenic CNS inflammation and demyelination during EAE progression in mice*

Previously, several studies demonstrated that certain miRNAs play an important role in the regulation of autoimmunity. One report found that *Mir223* regulates EAE though myeloid-derived suppressor cells. We wanted to investigate

whether endogenous *Mir223* levels affected the clinical symptoms of EAE in C57BL/6 mice immunized with the MOG[35–55] peptide as well as the mechanism involved. Interestingly, knockout of *Mir223* (*mir223*$^{-/-}$) significantly ameliorated the clinical symptoms of EAE compared with wild-type C57BL/6 mice (Figure 1A, B and C). In addition, disease severity, as assessed by the maximal and cumulative clinical score, was significantly decreased in *mir223*$^{-/-}$ mice (Figure 1D and E). These data suggest that endogenous *Mir223* levels affect the clinical outcome of EAE.

To characterize disease progression at the level of CNS injury, we performed a histological analysis of the lumbar spinal cord on day 15 post-immunization. At the peak of the acute phase of EAE, hematoxylin and eosin (H&E) and luxol fast blue staining showed that there was less infiltration of mononuclear cells and decreased demyelination in the lumbar spinal cords of *mir223*$^{-/-}$ mice compared with wild-type mice (Figure 1F and G). Thus, *Mir223* deficiency improves the pathological and clinical symptoms of EAE.

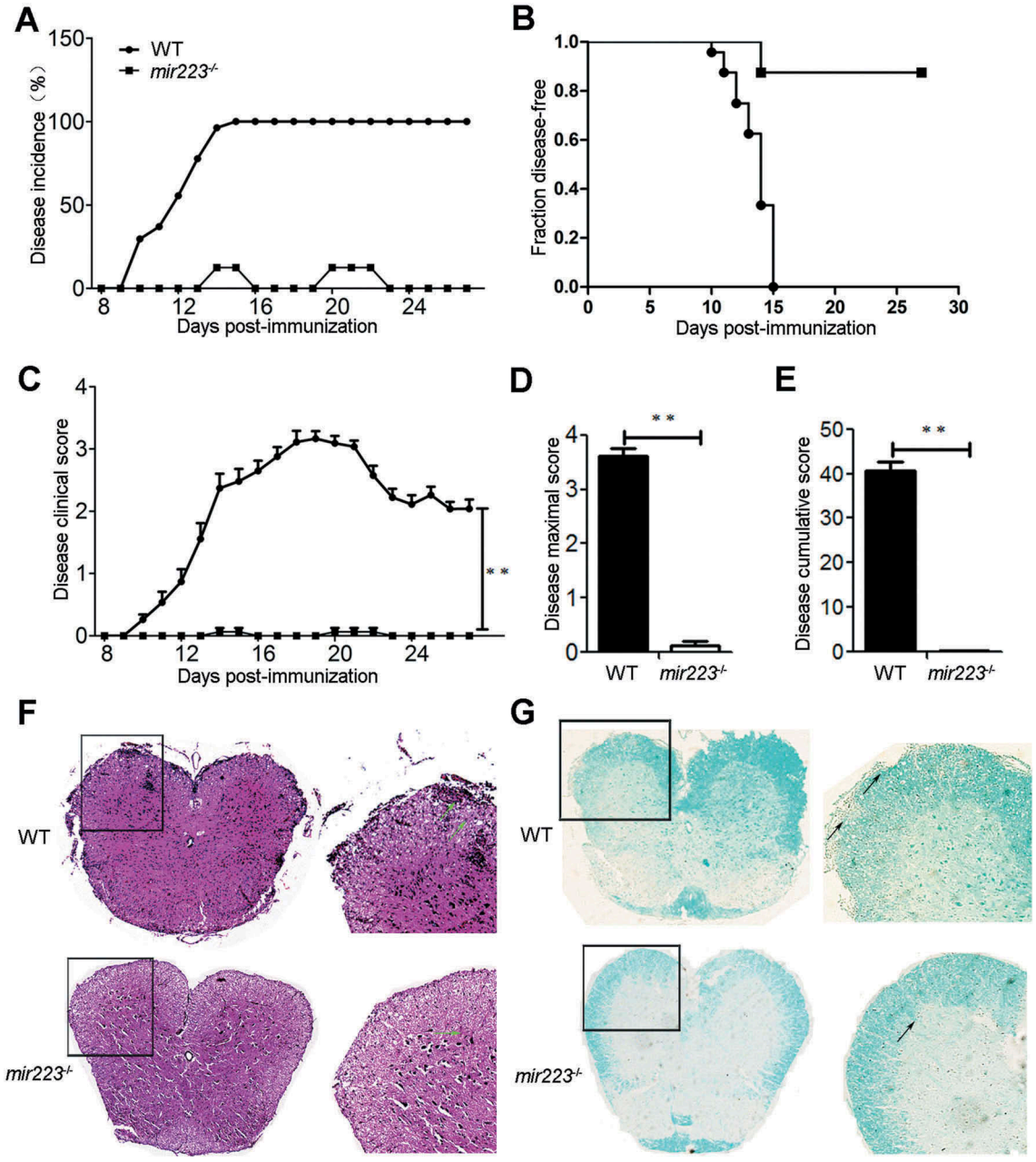

Figure 1. *mir223*$^{-/-}$ mice have alleviated EAE symptoms and decreased spinal cord inflammation and demyelination. EAE was induced with MOG[35–55] in female C57BL/6 mice (n = 12). The clinical scores of all of the EAE mice were assessed daily according to the same criteria for 28 continuous days. Incidence (**A**), disease onset (**B**), daily clinical scores (**C**), peak disease scores (**D**), and cumulative disease scores (**E**) were monitored. (**A**) The incidence of EAE (mice with clinical score ≥ 1 for 2 continuous days). The disease incidence is represented by the percentage of mice suffering from EAE. (**B**) Line graph depicts the EAE survival rate between WT and *mir223*$^{-/-}$ mice. (**C**) The clinical scores of all of the mice for 28 continuous days. (**D**) The mean maximum clinical scores. (**E**) The mean disease cumulative score. (**F**) H&E staining of representative spinal cord sections from *mir223*$^{-/-}$ mice and WT mice shows the infiltration of inflammatory cells in the white matter. (**G**) Luxol fast blue staining of intact myelin (blue) and demyelination (pink). The data are representative of at least 2 experiments with similar results.

Mir223 *deficiency augments autophagy and resting microglia in EAE mice*

Microglial cells play important roles in the regulation of EAE and MS. We assessed whether *Mir223* affects microglia in the CNS of EAE mice. Deficiency of *Mir223* decreased the infiltration of $ITGAM^+$ and $PTPRC^+$ cells and especially increased the $PTPRC^{low}$ and decreased the $PTPRC^{hi}$ cells. Overactive microglia can lead to profound neurological impairment. Here, we found that *Mir223* deficiency reduced the number of active microglia and macrophages ($ITGAM^+$ $PTPRC^{hi}$) but increased the number of resting microglia ($ITGAM^+$ $PTPRC^{low}$). There was also an augmentation of the ratio of the resting microglia vs the active microglia and macrophages in *mir223*$^{-/-}$ mice (Figure 2A and B).

There were considerably higher levels of LC3 protein in the microglia in the brains of *mir223*$^{-/-}$ mice than in wild-type mouse controls in the acute phase of EAE (Figure 2C). In contrast, BCL2 and BECN1/Beclin1 expression did not differ between the WT and *mir223*$^{-/-}$ mice (Figure 2D and **E**). It is possible that *Mir223* may regulate microglia autophagy though pathways other than BCL2 and BECN1, which remain unclear.

3-MA-mediated blockade of autophagy attenuates the protective effects of Mir223 *on EAE mice*

To determine the influence of autophagy on the effects of *Mir223* on the progression of MS *in vivo*, we examined neurobehavioral deficits in 3-MA- and vehicle-treated mice following MOG[35–55]-mediated induction of EAE. As shown in Figure 3, the disease course in the EAE mouse model was a chronic progressive-relapsing phenotype. *Mir223* deficiency significantly reduced the severity of neurobehavioral deficits, cumulative scores, and maximum neurological disability in EAE mice compared with WT mice. The effect of *Mir223* was abolished by 3-MA (10 mg/kg), an autophagy inhibitor (Figure 3A-3F), suggesting that *Mir223* plays a role in the progression of EAE at least partly through its effects on autophagy.

Mir223 *deficiency promotes autophagy in microphages and BV2 microglial cells stimulated with LPS*

Knockout of *Mir223* increased autophagy in microglia and resting microglia in the CNS during EAE progression. We differentiated macrophage cells from the bone marrow cells of wild-type C57BL/6 mice or *mir223*$^{-/-}$ mice *in vitro* to confirm that *Mir223* blocks autophagy in microglial cells upon LPS or starvation treatment. LC3 protein expression was increased in bone marrow-derived macrophage cells after stimulation with LPS or starvation, and ATG16L1 protein was mostly increased in *mir223*$^{-/-}$ mouse macrophages compared with those from wild-type mice (Figure 4A). Moreover, a *Mir223* inhibitor induced the production of autophagosomes and autolysosomes upon LPS stimulation in microglial BV2 cells (Figure 4B and C). These data indicate that endogenous *Mir223* can affect autophagy through the ATG16L1-LC3 pathway during EAE progression.

Mir223 *blocks LPS-induced autophagy in BV2 cells*

Recent advances have revealed a relationship between autophagy and innate immunity. Autophagy plays a crucial role in sustaining the balance between the beneficial and detrimental effects of immunity and inflammation [38]. It has been reported that LPS induces a non-typical autophagy pathway in BV2 microglia; however, the activation of the typical autophagy pathway using rapamycin inhibits the expression of NOS2 (nitric oxide synthase 2, inducible), IL6 (interleukin 6), and the cell death of microglia exposed to LPS [39]. Autophagy defects, resulting from nutrient deprivation or dysfunction of the autophagy-related proteins, may increase the degree of microglial activation and inflammation.

We then evaluated whether *Mir223* overexpression had an effect on LPS-induced autophagy. Past studies have suggested a link between toll-like receptor (TLR) signaling and autophagy in macrophages and other cell types via activation of downstream signaling pathways. TLR4 responds specifically to LPS stimulation. The autophagosome emanates from this signaling platform, and the membrane source for the generation of these initial structures is still debated. The most likely organelles to provide membranes include specialized phosphatidylinositol-3-phosphate-enriched endoplasmic reticulum domains and the Golgi apparatus. Here, we used the mitochondrial proteins TIMM23 and SQSTM1 (sequestosome 1) as a readout for autophagy. LPS-induced GFP-LC3 accumulation (Figure 5A and B), LC3 lipidation (Figure 5C) and TIMM23 degradation (Figure 5D) were decreased following *Mir223* overexpression. However, the expression of SQSTM1 did not cause any changes in BV2 cells during LPS stimulation. Cheng et al. found that *MIR181A* suppresses mitochondrial uncoupler-induced degradation of TIMM23 in SH-SY5Y human neuroblastoma cells, whereas SQSTM1 is not a reliable marker [40], and our results are consistent with these findings. Therefore, we concluded that *Mir223* inhibited LPS-induced autophagic activity in BV2 cells.

To confirm that *Mir223* inhibited autophagy-induced LC3 turnover and TIMM23 degradation, we performed similar autophagy assays in the presence or absence of the lysosomal inhibitor CQ. Indeed, addition of CQ led to the prominent accumulation of LC3-II and the degradation of TIMM23 in miR-CN-transfected cells upon LPS treatment, indicating the presence of normal autophagic flux under these conditions. However, because *Mir223* blocked autophagic vesicle generation, this inhibition-related accumulation of LC3-II and degradation of TIMM23 during LPS treatment was relatively decreased in BV2 cells overexpressing *Mir223* compared with mimic-expressing controls (Figure 5E and F).

Mir223 *blocked starvation-induced autophagy in BV2 cells*

To determine the role of *Mir223* in autophagy in microglia, we withdrew nutrition from BV2 cells transfected with *Mir223* mimics or mimic controls (Mim-CN) for 4 h to assess changes in autophagy-related genes and proteins. As shown in Fig. S1A and S1B, overexpression of *Mir223* significantly blocked starvation-induced GFP-LC3 accumulation. In line with these results, in cell extracts, starvation-activated lipid

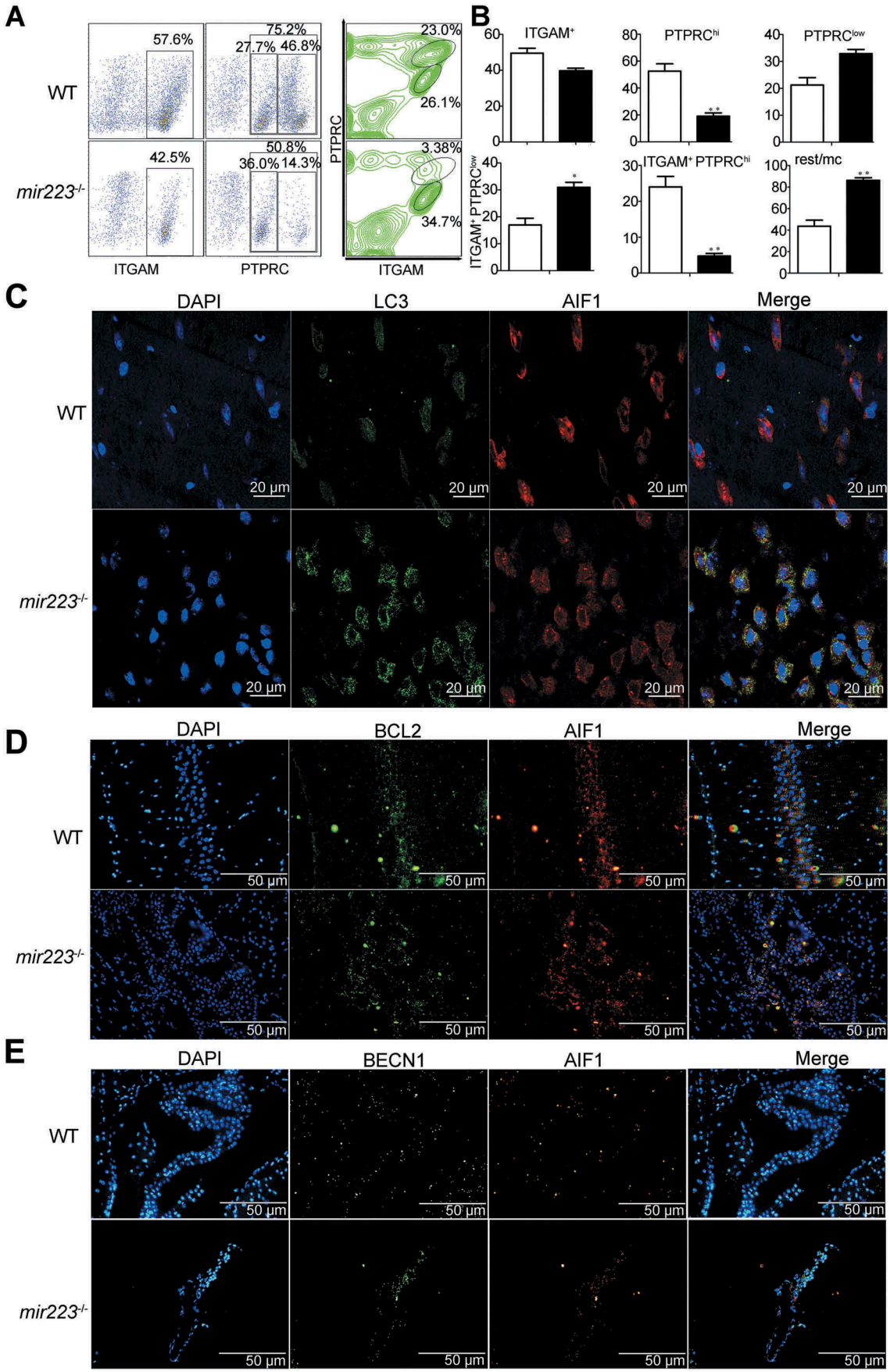

Figure 2. *Mir223* deficiency increased autophagy and resting microglia in the brains of EAE mice. (**A**) Flow cytometric analysis of microglia, demonstrating PTPRC and ITGAM cells isolated from the CNS of EAE mice (n = 6 mice per group), detected on the 15th day after the induction of EAE. The data are shown in a representative plot. (**B**) The absolute numbers of the cell subpopulations are shown; the black column is for *mir223*$^{-/-}$ mice. Rest, ITGAM^{+} PTPRC^{low}; mc, ITGAM^{+} PTPRC$^{hi\ and\ low}$. (**C**) Autophagy was measured in the brains of the mice. LC3 puncta were visualized by confocal imaging of microglia immunostained for LC3 and AIF1, followed by Alexa Fluor 488/555-conjugated secondary antibodies (green/red); nuclei were stained with DAPI. Representative images are shown. Scale bars: 20 μm. (**D**) and (**E**) BCL2 and BECN1 expression were visualized by fluorescence imaging of microglia. Scale bars: 50 μm.

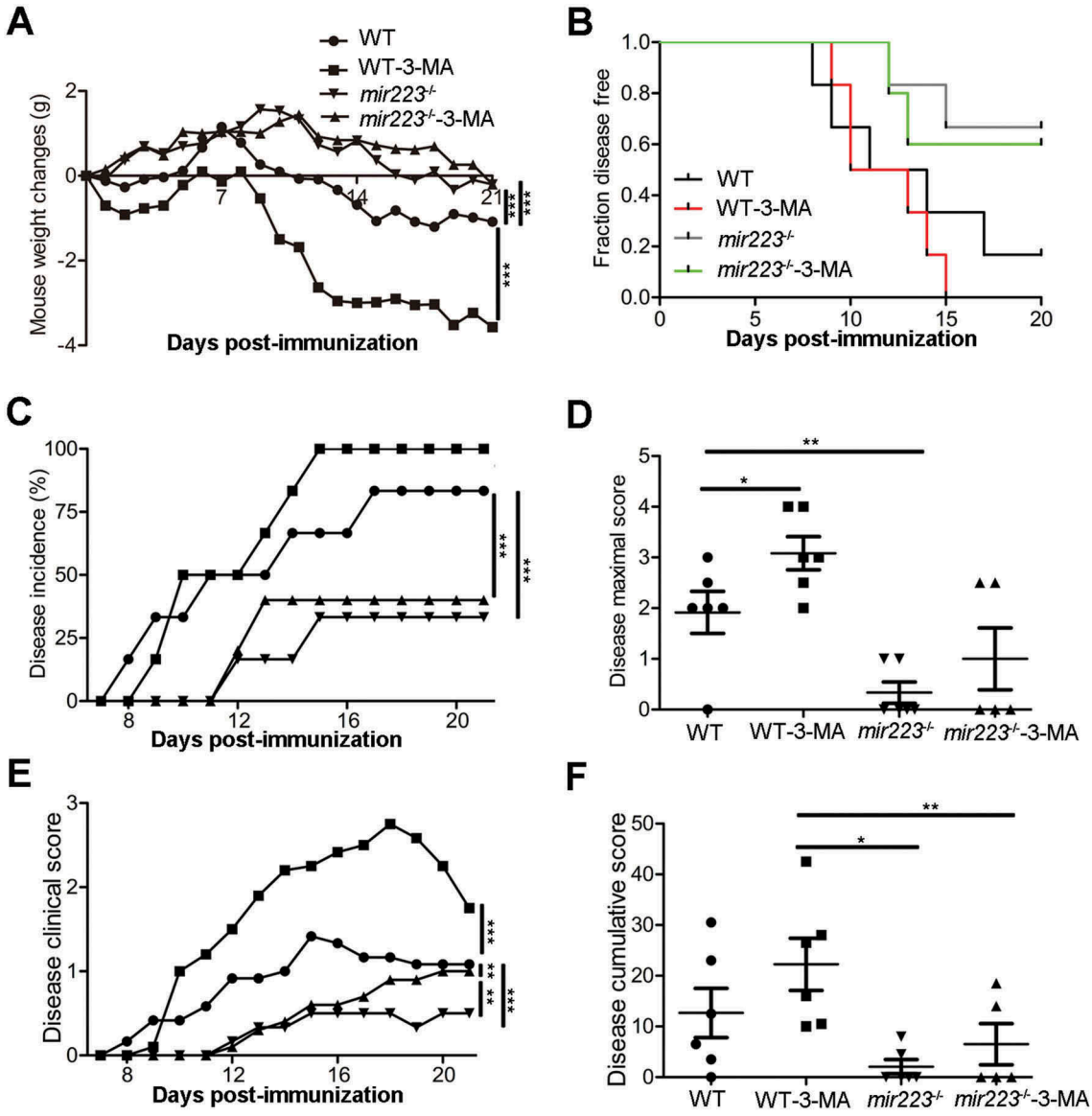

Figure 3. 3-MA-mediated blockade of autophagy attenuates the effects of *Mir223* on EAE mice. EAE was induced with MOG[35–55] in female C57BL/6 mice (n = 12). Mice were injected with 3-MA every day after immunization. The body weight and clinical scores of all of the EAE mice were assessed daily according to the same criteria for 21 continuous days. Body weight (**A**), disease onset (**B**), incidence (**C**), peak disease scores (**D**), daily clinical scores (**E**), and cumulative disease scores (**F**) were monitored.

conjugation of free LC3-I to the phagophore membrane to generate LC3-II was attenuated following transfection with *Mir223* mimics (Fig. S1C). Furthermore, degradation of the mitochondrial inner membrane protein TIMM23 following starvation was decreased in *Mir223*-transfected cell extracts (Fig. S1D). These results indicate that *Mir223* is a novel miRNA that controls autophagy.

To confirm that *Mir223* inhibition of autophagy-induced LC3 turnover and TIMM23 degradation also inhibited autophagic vesicle flux, we performed similar autophagy assays in the presence or absence of CQ. Indeed, addition of CQ led to the prominent accumulation of LC3-II and degradation of TIMM23 in miR-CN-transfected cells, pointing to the presence of normal autophagic flux under these conditions. However, because *Mir223* blocked autophagic vesicle generation, inhibition-related accumulation of LC3-II and degradation of TIMM23 during starvation were relatively lower in BV2 cells overexpressing *Mir223* compared with mimic controls (Fig. S1E and S1F).

Inhibition of endogenous Mir223 *increases autophagy upon LPS stimulation*

We then tested whether endogenous *Mir223* inhibition also had an effect on LPS-induced autophagy. We observed that the formation of LPS-dependent GFP-LC3 puncta was significantly increased (Figure 6A and B). Furthermore LC3-I to LC3-II conversion was stimulated (Figure 6C), and therefore, autophagy was accelerated in cells transfected with *Mir223*-inhibiting constructs compared with control antagomirs. Moreover, TIMM23 was degraded following the inhibition of endogenous *Mir223* upon LPS stimulation compared with controls (Figure 6D). Therefore, inhibition of endogenous

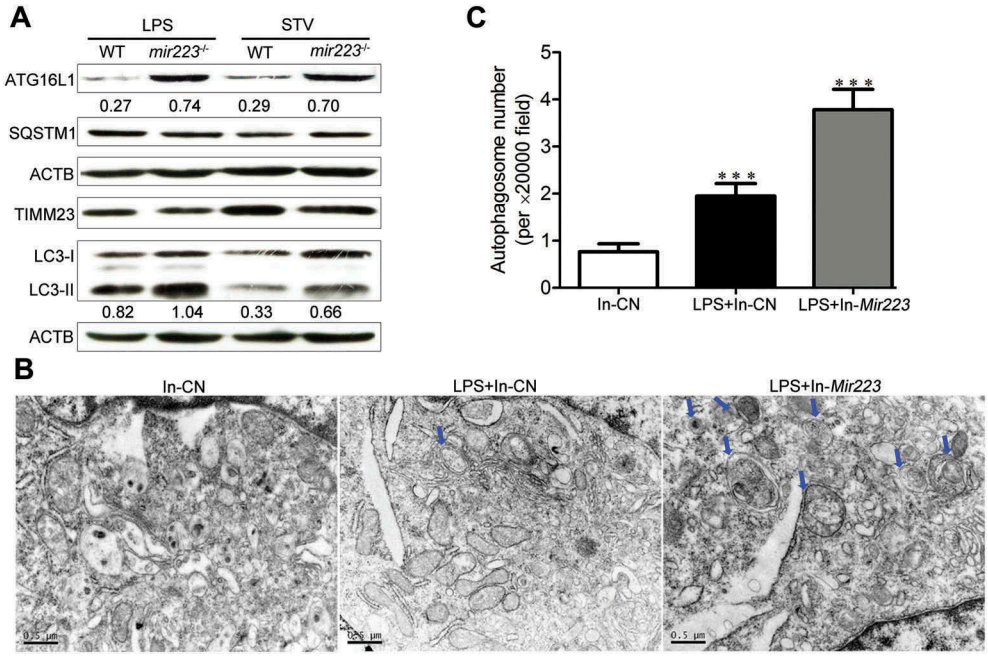

Figure 4. *Mir223* deficiency increases autophagy in primary macrophages and BV2 cells. (**A**) Macrophages were separated from the bone marrow of WT mice and *mir223*$^{-/-}$ mice. The cells were stimulated with LPS or starvation. Immunoblot analysis was performed for ATG16L1, SQSTM1, TIMM23, LC3 and ACTB. ATG16L1:ACTB and LC3-II:ACTB ratios are shown below the blots. (**B**) Deficiency of *Mir223* induces autophagic vacuoles in BV2 cells upon LPS stimulation. Scale bars: 0.5 μm. (**C**) Quantitative analysis of the number of autophagic vacuoles.

Mir223 using antagomirs led to the further stimulation of autophagic activity during LPS stimulation, indicating that endogenous *Mir223* contributes to the limitation of the LPS-activated autophagic response in BV2 cells.

To confirm that inhibition of *Mir223* increased autophagy-induced LC3 turnover and TIMM23 degradation, we performed similar autophagy assays in the presence or absence of CQ. Consistent with the above results, accumulation of LC3-II and degradation of TIMM23 during LPS stimulation was relatively higher in BV2 cells transfected with *Mir223* inhibitor compared with cells transfected with inhibitor controls (Figure 6E and F). Hence, attenuation of autophagic activity through inhibition of *Mir223* led to increased GFP-LC3 accumulation in BV2 cells when endogenous *Mir223* was blocked.

Inhibition of endogenous Mir223 *increases autophagy upon starvation*

Antagomirs, or anti-miRNAs, counteract miRNA effects by specifically inhibiting endogenous mature miRNAs. To test the effects of endogenous *Mir223* inhibition on autophagy, we transfected cells with *Mir223*-specific antagomirs (Inhibitor) or control antagomirs (In-CN) and analyzed autophagy under conditions of starvation or no starvation. We observed that the starvation-dependent formation of GFP-LC3 puncta was modestly but significantly increased (Fig. S2A and S2B) and LC3-I to LC3-II conversion was stimulated (Fig. S2C). Hence, autophagy was accelerated in cells transfected with *Mir223* inhibitor but not with control antagomirs. Moreover, TIMM23 degradation following starvation was more prominent after inhibition of *Mir223* compared with inhibitor controls (Fig. S2D). Therefore, inhibition of endogenous *Mir223* using antagomirs led to the further stimulation of autophagic activity during starvation, indicating that endogenous *Mir223* contributes to the limitation of stress-activated autophagic responses in microglial cells.

To confirm that inhibition of *Mir223* increased autophagy-induced LC3 turnover and TIMM23 degradation, we performed similar autophagy assays in the presence or absence of CQ. However, because inhibition of *Mir223* improved autophagic vesicle generation, accumulation of LC3-II and degradation of TIMM23 during starvation was relatively higher in BV2 cells transfected with *Mir223* inhibitor compared with those transfected with inhibitor controls (Fig. S2E and S2F). Hence, attenuation of autophagic activity through *Mir223* inhibition led to increased GFP-LC3 accumulation in BV2 cells in which endogenous *Mir223* was blocked.

The autophagy-related Atg16l1 *gene is a direct target of* Mir223

To determine the mechanism of *Mir223*-mediated autophagy inhibition, we searched for autophagy-related genes containing potential *Mir223* response elements in their 3' UTRs using the publicly available bioinformatics tools microRNA and miRTarBase. *Atg16l1* (GenBank accession number: NM_001205391.1, 138–163) was identified as a *Mir223* target by both bioinformatics tools. The predicted interaction between *Mir223* and the *Atg16l1* 3' UTR is shown in Figure 7A.

To further validate the effect of *Mir223* on *Atg16l1*, the region in the 3' UTR of the *Atg16l1* mRNA containing a potential *Mir223* response element was cloned into the 3' UTR of a luciferase vector. In parallel, we also created a

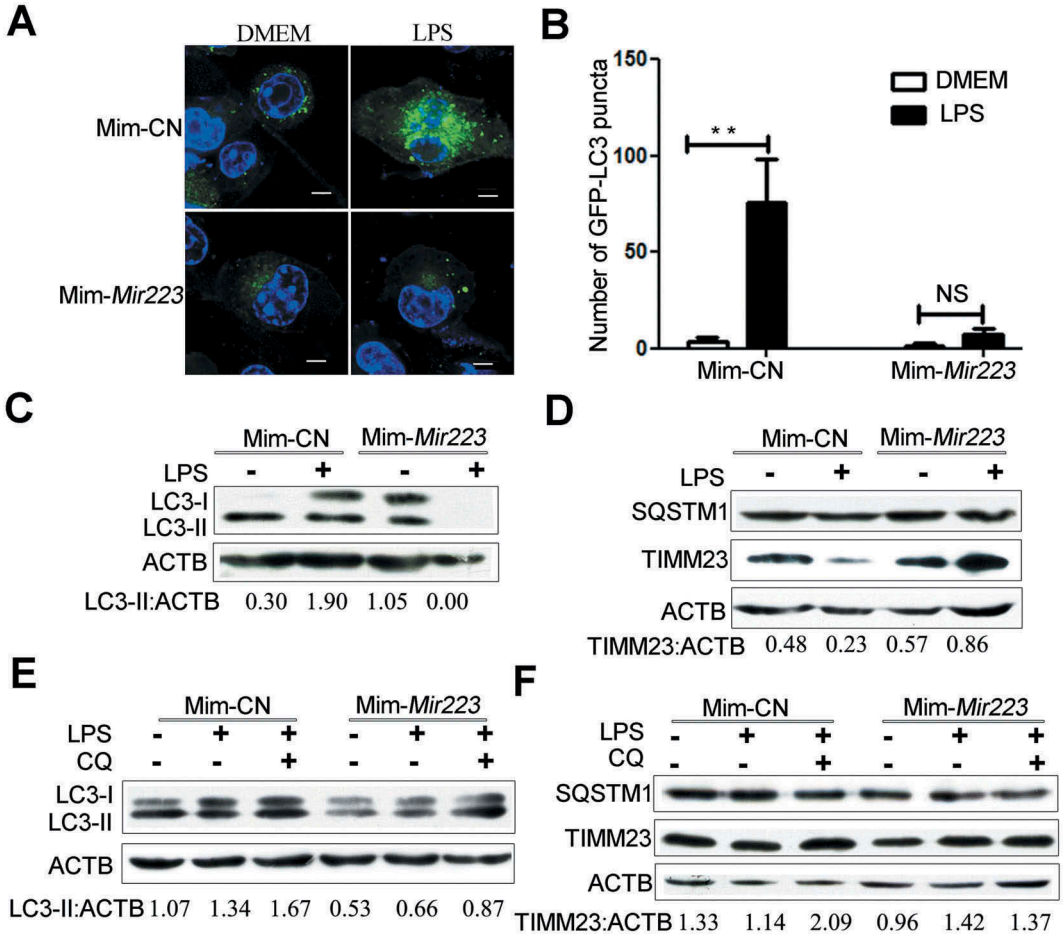

Figure 5. Overexpression of *Mir223* blocks lipopolysaccharide-induced autophagy in BV2 cells. (**A**) *Mir223* repressed the formation of starvation-induced GFP-LC3 puncta in BV2 cells. Stable GFP-LC3-expressing cells were cotransfected with mimics or Mim-CN, and autophagy was evaluated after LPS or control treatment for 4 h. Scale bar: 5 μm. (**B**) Quantitative analysis of the number of GFP-LC3 puncta per cell in (**A**). The data are presented as the mean± SEM; experiments were performed in triplicate (*$p < 0.05$, **$p < 0.01$; NS, not significant). (**C**) and (**D**) Western blot analysis of LC3, TIMM23, SQSTM1 and ACTB. (**E** and **F**) Autophagy was evaluated in the presence or absence of CQ with LPS or no LPS treatment for 4 h. Western blot analysis of LC3, TIMM23, SQSTM1 and ACTB. Densitometric ratios were quantified using ImageJ software. LC3-II:ACTB and TIMM23:ACTB ratios from immunoblots are shown from 3 independent experiments. ACTB was used as the loading control.

mutant version of this construct by introducing base changes to the crucial binding residues, primarily in the *Mir223* seed sequence-binding region (Figure 7B). Cotransfection of *Mir223* mimics together with the wild-type luciferase vector in 293T cells resulted in a significant decrease in luciferase activity compared with control levels (Figure 7C, target). In contrast, *Mir223* had no significant effect on the levels of luciferase activity compared to the mutant construct; here, the luciferase activity was similar to control levels (Figure 7C, mutant). These results showed that *Mir223* controlled the levels of ATG16L1 by directly targeting the above-described MRE in the 3' UTR region of the *Atg16l1* gene.

The expression of *Mir223* was decreased by qPCR in BV2 cells following transfection with *Mir223* inhibitor but not with In-CN in the presence or absence of LPS stimulation (Figure 7E). To confirm the bioinformatics-based predictions, we performed immunoblot assays of control- or *Mir223* mimic-transfected cell extracts using an ATG16L1-specific antibody. Indeed, ATG16L1 protein levels were decreased in BV2 cells overexpressing *Mir223* under starvation conditions (Figure 7F). Conversely, introduction of the *Mir223* antagomir, but not control antagomirs, resulted in an increase in ATG16L1 protein levels in BV2 cells during starvation (Figure 7G). *Mir223* expression also affected target transcript levels in cells. An increase in *Atg16l1* mRNA levels was observed by qPCR in BV2 cells following transfection with *Mir223* inhibitor but not with In-CN (Figure 7H).

Overexpression of ATG16L1 abrogated mir223*-mediated suppression of autophagy*

To further confirm that downregulation of ATG16L1 was responsible for the autophagy-related effects of *Mir223*, we performed 'rescue experiments'. In these experiments, *Atg16l1* was overexpressed by a plasmid lacking a *Mir223* binding site; it was therefore resistant to *Mir223*-mediated downregulation of *Atg16l1*. Hence, although *Mir223* overexpression decreased endogenous ATG16L1 protein levels significantly, cells cotransfected with the *Mir223* mimics and an *Atg16l1* plasmid lacking the *Mir223* binding site possessed near-physiological levels of total ATG16L1 protein (Figure 8A and B). Under these conditions, the *Mir223*-mediated suppression of

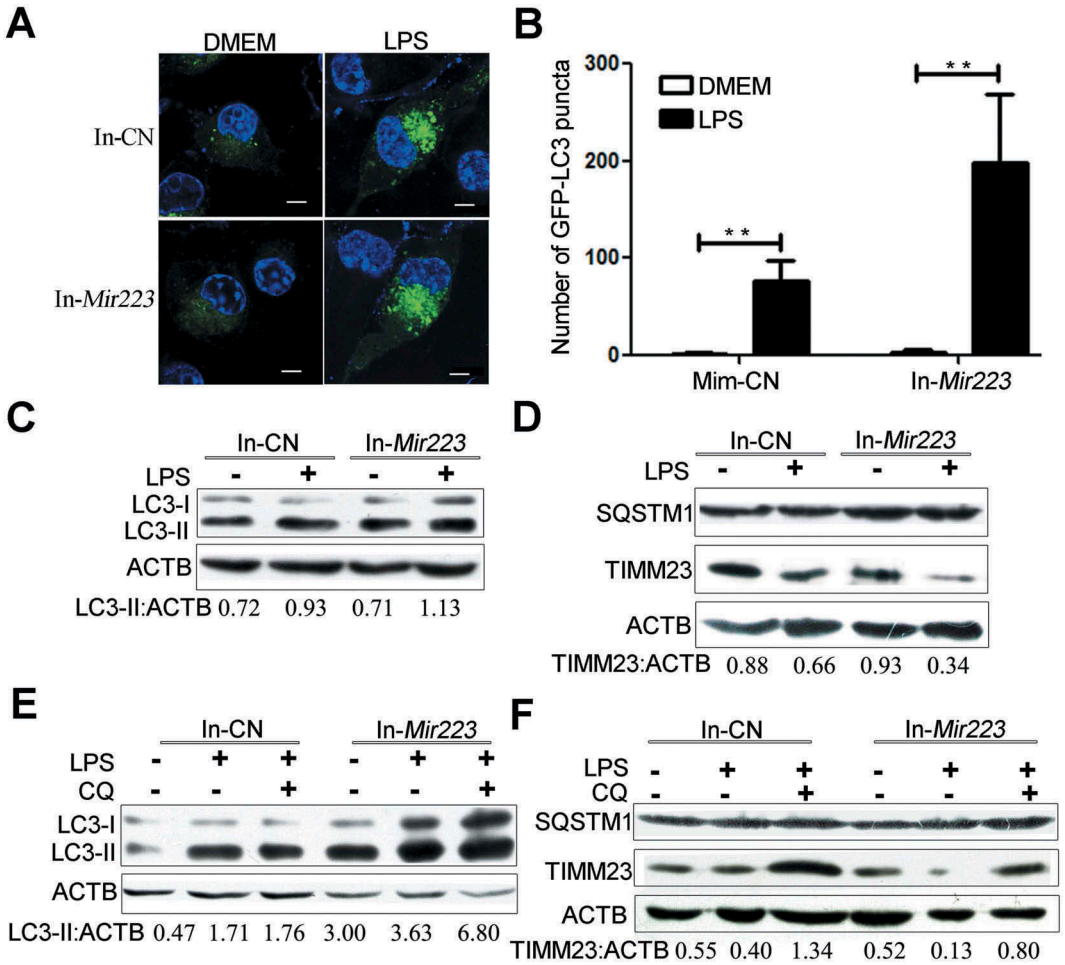

Figure 6. Inhibition of endogenous *Mir223* increases autophagy upon LPS stimulation. (**A**) *Mir223* repressed the formation of starvation-induced GFP-LC3 puncta in BV2 cells. Stable GFP-LC3-expressing cells were cotransfected with inhibitor (In-*Mir223*) or In-CN, and autophagy was tested after LPS or control treatment for 4 h. Scale bar: 5 μm. (**B**) Quantitative analysis of the number of GFP-LC3 puncta per cell in (**A**). The data are presented as the mean± SEM; experiments were performed in triplicate (*$p < 0.05$, **$p < 0.01$). (**C** and **D**) Western blot analysis of LC3, TIMM23, SQSTM1 and ACTB. (**E** and **F**) Autophagy was tested in the presence or absence of CQ with LPS or control treatment for 4 h. Western blot analysis of LC3, TIMM23, SQSTM1 and ACTB. Densitometric ratios were quantified using ImageJ software. LC3-II:ACTB and TIMM23:ACTB ratios from immunoblots are shown from 3 independent experiments. ACTB was used as the loading control.

autophagy observed during starvation-induced autophagy was reversed upon co-expression of the ATG16L1 protein (Figure 8C and D). In other words, introduction of the ATG16L1 protein was sufficient to return autophagy back to normal levels even in the presence of the *Mir223* mimics. These results demonstrated that *Atg16l1* was the target of *Mir223* for the suppression of autophagy.

Mir223 *regulation of autophagy is independent of the BCL2 and PPARG pathways*

The antiapoptotic protein BCL2 is involved in autophagy regulation through sequestration of the autophagy-related protein BECN1. In our study, inhibition or overexpression of *Mir223* did not significantly affect the levels of BCL2 protein under LPS stimulation conditions in BV2 cells (Fig. S3A and S3B). Therefore, we propose that autophagy regulation by *Mir223* did not proceed through BCL2. We also examined whether there are other autophagy-related targets of *Mir223*. Because *Mir223* can regulate IFNG (interferon gamma) by directly targeting PPARG (peroxisome proliferator activated receptor gamma), and PPARG plays an important role in the activation of macrophage cells and in neuronal autophagy during cerebral ischemia-reperfusion injury[41], we wondered whether the PPARG pathway would be affected by *Mir223* overexpression. To assess the effect of *Mir223* on PPARG, we analyzed the protein levels of PPARG. Although under basal/fed conditions, inhibition or overexpression of *Mir223* did not have a differential effect on PPARG expression between cells transfected with *Mir223* inhibitor or mimics and control cells, PPARG expression vanished following autophagy activation via LPS stimulation (Fig. S4). Therefore, we concluded that although it is possible that other targets of *Mir223* could contribute to its biological effects, ATG16L1 appears to be the major and rate-limiting autophagy-related target of *Mir223*.

Discussion

In this study, we introduced *Mir223* as a novel autophagy regulator. *Mir223* deficiency significantly reduced the severity of neurobehavioral deficits, cumulative scores, and maximum

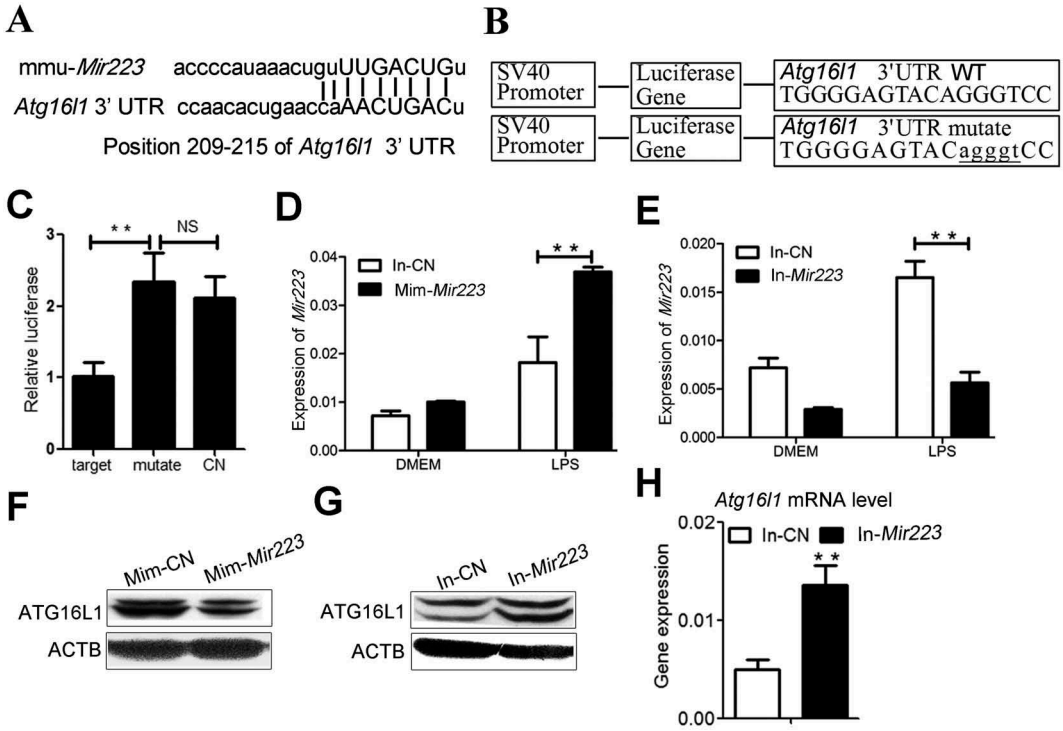

Figure 7. *Atg16l1* as a direct target of *Mir223*. (**A**) The *Mir223* target sequence in the 3′ UTR of *Atg16l1* in mice. (**B**) A scheme representing the luciferase constructs with the wild-type (WT) or mutant 3′ UTR *Mir223* MRE sequences of *Atg16l1*. Mutations are marked in lower-case letters and underlined. (**C**) Normalized luciferase activity in lysates from 293T cells co-transfected with wild-type or mutant *Atg16l1*-luciferase constructs and *Mir223* mimics or Mim-CN (mean± SEM, n = 3, *$p < 0.05$, **$p < 0.01$). (**D** and **E**) BV2 cells were cotransfected with *Mir223* Mim-CN, mimics, In-CN or inhibitor and starved for 4 h. Quantitative PCR (qPCR) analysis of *Atg16l1* mRNA levels is shown. (**F** and **G**) BV2 cells were cotransfected with *Mir223* Mim-CN, mimics, In-CN or inhibitor and starved for 4 h. The ATG16L1 protein level was tested by immunoblotting. ACTB was used as the loading control. (**H**) Quantitative PCR (qPCR) analysis of *Atg16l1* mRNA levels in In-CN- or inhibitor-transfected BV2 cells. The data are expressed as the mean± SEM; experiments were performed in triplicate (*$p < 0.05$, **$p < 0.01$). The data were normalized to *Gapdh* mRNA.

neurological disability in EAE mice compared with WT mice. The effect of *Mir223* was abolished by the autophagy inhibitor 3-MA, suggesting that *Mir223* plays a role in EAE progression at least partly through autophagy. Here, we found *mir223*$^{-/-}$ reduced the number of active microglia and macrophages and simultaneously increased the number of resting microglia. Moreover, there were considerably higher levels of LC3 protein in microglia in the brains of *mir223*$^{-/-}$ mice than in wild-type controls during the acute phase of EAE. Overexpression of *Mir223* inhibited GFP-LC3 accumulation, LC3-I to LC3-II conversion and TIMM23 degradation in BV2 cells. These results were validated by stimulation of BV2 cell autophagy upon starvation and LPS treatment. Additionally, antagonist-mediated suppression of endogenous cellular *Mir223* accelerated the autophagic response. Together, these data showed that *Mir223* is a key player in controlling autophagy. We identified ATG16L1 as a target of *Mir223* through miRNA gene blast and luciferase reporter analysis of the MRE found in the 3′ UTR region of the *Atg16l1* gene. The results we obtained in this study may be summarized in a mechanistic model as follows (Figure 8E): A certain portion of cellular ATG16L1 protein can form functional ATG12–ATG5-ATG16L1 complexes, followed by LC3 lipidation and autophagy activation. The presence of *Mir223* under stimulation leads to the downregulation of ATG16L1 protein levels below the threshold and therefore results in a decrease in LC3 lipidation and inhibition of autophagic activity. Thus, inhibiting *Mir223* can regulate autophagy and improve/limit uncontrolled or potentially harmful autophagic activity in cells.

An increasing number of studies have revealed novel knowledge regarding autophagy, and our understanding of autophagy in autoimmune inflammation is rapidly being updated. It is principally thought that autophagy plays an important role in protecting neurocytes from inflammation. BCL2 and BECN1 are important for controlling cellular autophagy in response to environmental stress or treatment with BH3 peptidomimetics. In this study, we found that *Mir223* did not affect BCL2 and BECN1 expression during EAE progression or in BV2 cells upon LPS stimulation. These results suggested that *Mir223* regulates autophagy through other pathways.

Multiple genetic studies have implicated the autophagy-related gene *Atg16l1* in this regulatory process, and luciferase reporter assays have indicated that *MIR106B* and *MIR93* target *ATG16L1* mRNA [42]. Zhai et al. reported miRNA-mediated regulation of ATG16L1 in colonic epithelial cells as well as Jurkat T cells. Dual-luciferase reporter assays found that *MIR142* is a key miRNA that regulates *ATG16L1* by targeting the 3′ UTR. The study revealed that *MIR142* is a new autophagy-regulating small molecule that acts by targeting *ATG16L1*, indicating a role of *MIR142* in intestinal inflammation and Crohn disease[43]. Other researchers have found that ATG16L1 is also a target gene regulated by *Mir20a* [44,45]. Bacillus Calmette-Guérin infection of macrophages

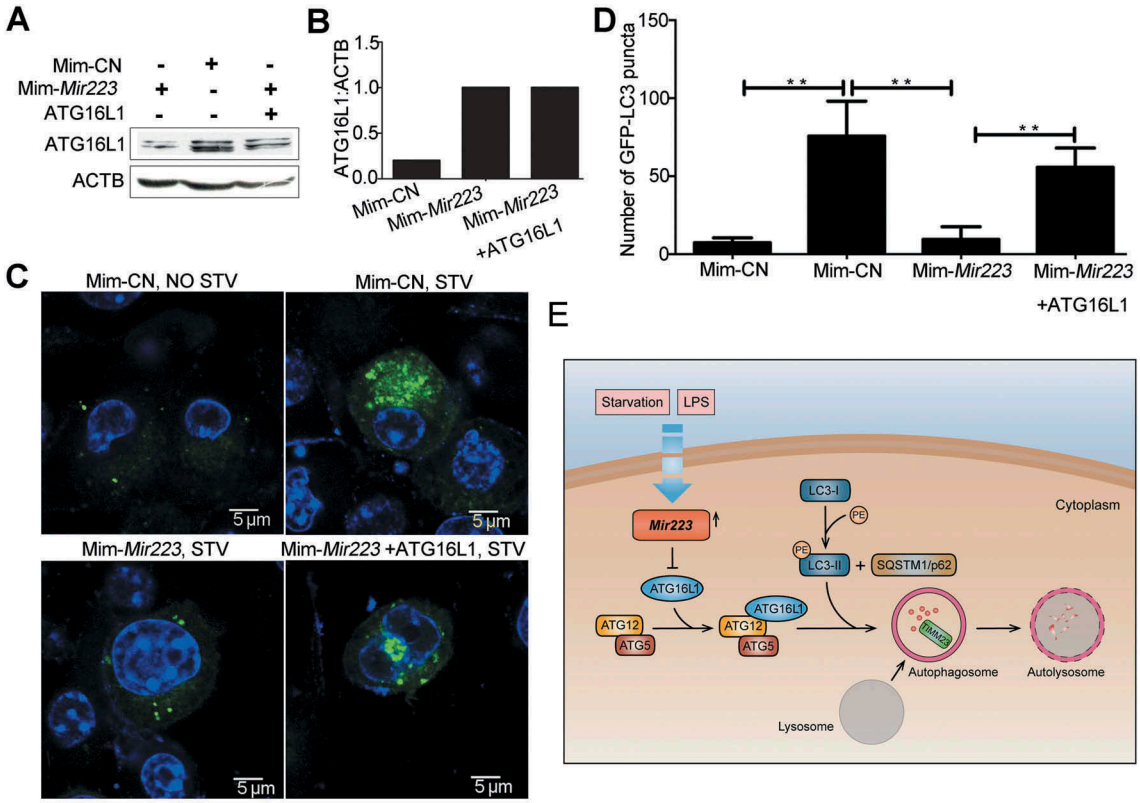

Figure 8. ATG16L1 protein overexpression abrogates *Mir223*-mediated autophagy suppression. BV2 cells were cotransfected with *Mir223* mimics or Mim-CN and ATG16L1 expression plasmid lacking the *Mir223* target region. (**A**) Cells were starved for 4 h. Immunoblot analysis of ATG16L1 and ACTB is shown. (**B**) ATG16L1:ACTB ratios. (**C**) Formation of GFP-LC3 puncta before or after starvation for 4 h. Scale bar: 5 μm. (**D**) Quantitative analysis of GFP-LC3 puncta (mean± SEM, n = 3, $^{*}p < 0.05$, $^{**}p < 0.01$). (**E**) Model of the effect of *Mir223* regulation of autophagy through direct targeting of *Atg16l1*.

results in enhanced expression of *Mir20a*, which decreases the expression levels of LC3-II and the number of LC3 puncta in macrophages. In addition, *Mir20a* promotes Bacillus Calmette-Guérin survival in macrophages, whereas transfection with a *Mir20a* inhibitor has the opposite effect. Moreover, transfection with a *Mir20a* mimic leads to a significant reduction in the number of autophagosomes per cellular cross-section, but transfection with a *Mir20a* inhibitor increases the number of autophagosomes per cellular cross-section [46]. In ischemic kidney injury and HK-2 cells under hypoxic conditions, the expression of punctate LC3 and ATG16L1 is increased and *Mir20a* expression is decreased. The 3' UTR luciferase reporter assays indicate that *Mir20a* targets *Atg16l1* mRNA. Overexpression of *Mir20a* and antagoMir20a also confirm these results [44]. In osteoclasts, a dual-luciferase reporter assay revealed that *Mir20a* directly targets *Atg16l1* by binding to its 3' UTR [45].

We identified ATG16L1 as a target of *Mir223* through miRNA gene blast and luciferase reporter analysis of the MRE found in the 3' UTR region of the *Atg16l1* gene, and we found that introduction of mutations to this sequence abolished the effect of *Mir223*. We showed that *Mir223* overexpression attenuated ATG16L1 protein and mRNA levels, and more importantly, reintroduction of ATG16L1 protein in the presence of *Mir223* mimics blocked autophagy. Therefore, our results established ATG16L1 as an important target of *Mir223* during autophagy regulation. Whether autophagy inhibits or enhances inflammatory cell infiltration depends on the related signaling pathways targeted by different stimulators and cells. Moreover, further studies are needed to reveal the role of autophagy during autoimmune inflammatory reactions.

Mir223 was previously shown to be involved in various biological processes, such as development, differentiation, hematopoiesis, and immune modulation. In fact, autophagy has also been described as an important regulator of similar physiological events [47–50]. Study of the effects of autophagy on these processes could provide valuable information about the importance of *Mir223*. *Mir223* was upregulated in the blood and lung parenchyma of tuberculosis (TB) patients and in TB-infected mice. Deletion of *Mir223* renders TB-resistant mice highly susceptible to acute lung infection [51]. The apoptosis rate of peripheral blood macrophages is decreased in active TB patients compared with healthy controls. Transfection of human macrophages (TDMs and MDMs) with *MIR223* inhibits macrophage apoptosis. Moreover, researchers found that *MIR223* directly suppresses FOXO3 (forkhead box O3), and FOXO3 plays a critical role as a mediator of the biological effects of *MIR223* in macrophage apoptosis [52]. In macrophages, *MIR223* may regulate apoptosis by directly targeting *FOXO3*. Activation of CNR2 (cannabinoid receptor 2, [macrophage]) can ameliorate the pathogenesis of EAE, whereas deleting *Cnr2* decreases LC3-II/LC3-I and BECN1 expression and increases CASP1 (caspase 1) activation and IL1B production in EAE mice. In contrast activation of CNR2 with the specific agonist HU-308 induces inverse effects. At the same time, one study reported that HU-

308 promotes autophagy in BV2 microglia. These results demonstrate that CNR2 plays a protective role in EAE by promoting autophagy [53]. In our results, we also found that *Mir223* expression was increased in the spleen and CNS during EAE progression (unpublished data). At the same time, autophagy was repressed in brain microglial cells, whereas *Mir223* deficiency increased LC3 expression and ameliorated EAE pathogenesis.

Some researchers have identified an increase in autophagy during the progression of autoimmune disease. Systemic lupus erythematosus is an autoimmune disease, and overexpression of TLR7 has been found to be associated with this disease. We ablated autophagy in *Tlr7*-transgenic (Tg) mice, and, in the absence of autophagy, these mice were cured of lupus. This was also supported by the survival of autophagy-deficient mice compared to the Tg(Tlr7)1Boll/Tlr7.1 Tg mice [54]. Rheumatoid arthritis (RA) is a kind of autoimmune disease that involves dysregulation of $CD4^+$ T cells. One report demonstrated that autophagy is significantly increased in $CD4^+$ T cells from RA patients and that increased autophagy is also observed in activated $CD4^+$ T cells. Increased resistance to apoptosis is also observed in $CD4^+$ T cells from RA patients. These results provide novel insight into the connection between the pathogenesis of RA and autophagy [55].

Autophagy deficiency is associated with many diseases. Therefore, autophagy has been proposed as a cell-protective mechanism. Similarly, we observed that inhibition of *Mir223* can ameliorate the pathogenesis of EAE by increasing autophagy in brain microglial cells. Further research also showed that intraperitoneal injection of 3-MA in mice can aggravate the pathogenesis of EAE. Therefore, changes in the *Mir223* level might modulate autophagy and affect the clinical pathogenesis of EAE. Further studies are required to explore the contribution of *Mir223* expression to other autoimmune diseases regulated by macrophages.

Materials and methods

Animal experiments

Female C57BL/6 mice aged 7–8 weeks were purchased from the Academy of Military Medical Science (Beijing, China). *mir223*$^{-/-}$ mice were kindly provided by Fei Gao's lab (Institute of Zoology, Chinese Academy of Sciences, Beijing), which is a global knockout. The *Mir223* gene is located on the X chromosome. The animals were housed and fed in a specific pathogen-free animal facility at the Experimental Animal Center of Tianjin Medical University (Tianjin, China). The experiments were performed in accordance with the guidelines for animal care and were approved by the Animal Ethics Committee of Tianjin Medical University (Tianjin, China).

For EAE induction, the C57BL/6 female mice were immunized (subcutaneously) with 200 μg of myelin oligodendrocyte glycoprotein (MOG residues 35–55). The peptide sequence was Met-Glu-Val-Gly-Trp-Tyr-Arg-Ser-Pro-Phe-Ser-ArgVal-Val-His-Leu-Tyr-Arg- Asn-Gly-Lys, and the purity was > 95% (CL Bio-Scientific Co., Ltd.). The immunization was performed by mixing the MOG[35–55] peptide with complete Freund's adjuvant containing 500 μg of heat-killed H37Ra, a *Mycobacterium tuberculosis* strain (Difco Laboratories, 231,141). Pertussis toxin (200 ng) (List Biological Laboratories, 180) in PBS (BBI Life Sciences, A610100-0001) was administered intraperitoneally on the day of immunization and again after 48 h. For inhibition of autophagy, mice were treated with 3-MA (10 mg/kg; Sigma, M9281) daily. The mice were weighed and examined daily for disease symptoms, which were assessed using the following standard score system: 0, no obvious changes in motor functions; 1.0, limp tail; 2.0, limp tail and wobbly gait; 3.0, bilateral hind limb paralysis; 4.0, complete hind limb and partial forelimb paralysis; and 5.0, death [56].

Histopathology and immunohistochemistry

The lumbar spinal cords from the female C57BL/6 mice and *mir223*$^{-/-}$ mice (n = 6) were perfused transcardially with 4% (weight:volume) paraformaldehyde and were then dissected and post-fixed for 48 h. The spinal cord paraffin sections (7 μm) were stained with H&E to detect inflammatory cell infiltration and with luxol fast blue (Alfa Aesar,1328–51-4) to assess demyelination.

The brains from the wild-type C57BL/6 mice and *mir223*$^{-/-}$ mice (n = 6) were perfused transcardially with 4% (weight: volume) paraformaldehyde and then were dissected and post-fixed for 48 h. The brain paraffin sections (7 μm) were stained with DAPI (Thermo Fisher Scientific, 00–4959-52), LC3A/B (Cell Signaling Technology, 12,741), BCL2 (Abcam, ab32124), BECN1 (Cell Signaling Technology, 3495), AIF1/IBA1 (allograft inflammatory factor 1) (Abcam, ab107159) and Alexa Fluor 488 (Proteintech, SA00006-2) and Alexa Fluor 546 (Thermo Fisher Scientific, A11056) secondary antibody conjugates (green and red, respectively).

Intracellular cytokine staining

The single-cell suspensions were isolated from the brain and spinal cords of WT or *mir223*$^{-/-}$ EAE mice by grinding and filtering the tissue through a cell strainer. Then, the macrophages and microglial cells were separated by Percoll (GE Healthcare Bio-Sciences AB, 17–0891-09) gradient centrifugation at 630g for 25 min. The cell surface markers were assessed with APC-conjugated anti-mouse PTPRC antibody (eBioscience, 17–0451-82) and PE-conjugated anti-mouse ITGAM (eBioscience, 12–0112-82). Nonspecific staining was monitored with isotype antibody controls PE IgG2b (eBioscience, 12–4031-82) and APC IgG2b (Sungene biotech, R20022-11A). The cells were analyzed by BD FACS Canto II (BD Biosciences, USA), and the acquired data were analyzed using FlowJo software.

Separation of macrophages from bone marrow

Femurs and tibias, removed from wild-type C57BL/6 mice and *mir223*$^{-/-}$ mice immediately after they were sacrificed, were cleaned of muscle tissues, placed in a petri dish with 70% ethanol for 2–3 min and washed twice in sterile culture medium. Bone ends were cut, and the marrow was flushed out into a new petri dish with 10 ml of RPMI (Gibco, 31,800–022). Cells

were then washed and resuspended in RPMI supplemented with 10% fetal bovine serum (FBS; Gibco, 10,099,141) and 10 ng/ml CSF1/M-CSF (Peprotech, 315–02). After an adhesion step of 5 days on a plastic dish at 37°C and 5% CO_2, the cells were stimulated with LPS (Sigma, L4516) or starvation for 4 h.

Cell culture and treatment

The mouse microglial cell line BV2 was obtained from the Cell Resource Center, IBMS, CAMS/PUMC (Beijing, China). The cell line was grown in Dulbecco's modified Eagle's medium (Gibco, 12,800–017), supplemented with 10% FBS, and 10 U/ml penicillin-streptomycin (Gibco, 15,140–122). The cells were cultured in a 5% CO_2 humidified incubator at 37°C. LPS and hydroxychloroquine (CQ; Sigma, H0915) were dissolved in DMEM and dimethyl sulfoxide (Solarbio, D8370), separately. To induce autophagy, cells were treated with starvation or LPS for 4 h.

Transmission electron microscopy

The cells were fixed with ice cold 2.5% glutaraldehyde (pH 7.4). After being washed 3 times with 0.1 M phosphate buffer, pH 7.4, the cells were fixed with 1% osmium tetraoxide for 1 h. The samples were dehydrated in a graded series of ethanol concentrations and embedded in Spurr resin (TED PELLA, 18,300–4221). The ultrathin sections were cut to a thickness of 70 nm and then double-stained with uranyl acetate and lead citrate. The number of autophagic vacuoles was determined for a minimum of 100 cells. The samples were examined and photographed with a JEM-1230 transmission electron microscope (JEOL, Japan) by FCEN Company (Shanghai Fucheng Biological Technology Co., Ltd., China).

Target prediction for miRNA

miRNA targets were identified using the publicly available bioinformatics tools microRNA (http://www.microrna.org/microrna/home.do) and miRTarBase (http://mirtarbase.mbc.nctu.edu.tw/).

MicroRNA, siRNA, plasmid and transfection

Mir223 mimics, control mimics (Mim-CN), *Mir223* inhibitor (a *Mir223*-specific antagomir), and control inhibitor (In-CN) were synthesized by Ribobio (Guangzhou, China). For the dual-luciferase assay, the MRE found in the 3' UTR region of the *Atg16l1* mRNA and its mutated version were cloned into a pmirGLO-control vector (Promega, E1741) at the 3' region of the luciferase gene using the following linker primers: *Atg16l1* wild-type primers. 5'-CGTAGCGGCCGCTAGTTGGGGAGTACAGGGTCCCT-3' and 5'-CTAGAGGGACCCTGTACTCCCCAACTAGCGGCCGCTACGAGCT-3' and *Atg16l1* mutant primers 5'-CTAGAGGGACCCTGTACTCCCCAACTAGCGGCCGCTACGAGCT-3' and 5'-CTAGAGGGTGGGAGTACTCCCCAACTAGCGGCCGCTACGAGCT-3'.

Transient transfection of BV2 cells was performed using either polyethyleneimine (Polysciences Inc., 23,966) or Lipofectamine® RNAi Max reagent (Invitrogen, 13,778–075) according to the manufacturer's instructions. Briefly, 293T cells were harvested and lysed 48 h post-transfection. Firefly and Renilla luciferase activities were measured using a dual-luciferase-reporter assay system (Promega, E1910). The results were evaluated through normalization of the firefly luciferase activity with the Renilla luciferase activity.

GFP-LC3 analyses

Forty-eight h after cotransfection of *Mir223* mimics, Mim-CN, inhibitor, In-CN and GFP-LC3 (HANBio, China), BV2 cells were incubated for 4 h in EBSS medium or in DMEM-FBS containing 500 ng/ml LPS for 4 h. Cells were fixed in 4% formaldehyde for 10 min, washed with PBS, mounted and inspected under 100 × magnification using a BX60 fluorescence microscope (Olympus, Germany), followed by image analysis with ImageJ software (National Institutes of Health, Bethesda, MD, USA) after quantifying pixel (200 pixels) intensities of both cellular compartments and subtracting background fluorescence. At least 100 GFP-positive cells per condition were counted, and the graphs were plotted as the number of GFP-LC3 puncta per cell.

Western blot analyses and antibodies

Protein extraction was performed with RIPA buffer supplemented with complete protease inhibitor cocktail (Roche, 04–693-131–001) and 1 mM phenylmethylsulfonyl fluoride (Sigma-Aldrich, P7626). The lysates were clarified by centrifugation at 3600 g for 20 min at 4°C, and the protein concentration was quantified using the BCA protein assay kit (Applygen Technologies Inc., P1511). Cell extracts (5–10 μg) were denatured for 5 min in 5 × SDS-PAGE loading buffer (CWBIO, cw0027), separated on 10% SDS-polyacrylamide gels and transferred onto PVDF membranes (Roche, 03010040001). Following blocking in 5% nonfat milk in TBST (20 mM Tris base, 137 mM NaCl, 0.1% Tween 20 [SbaseBio, A336], pH 7.4) for 1 h at room temperature, membranes were incubated in 5% milk-TBST solutions containing the following primary antibodies: anti-ATG16L1 (Cell Signaling Technology, 8089), anti-LC3 (Cell Signaling Technology, 12,741), anti-SQSTM1/p62 (Cell Signaling Technology, 5114), anti-TIMM23 (Proteintech, 11,123–1-AP), anti-ACTB/β-actin (Vazyme, Ab101-01), anti-BCL2 (Abcam, ab32124) and anti-PPARG (Proteintech, 22,061–1-AP) at 4°C overnight. Then, secondary anti-mouse or anti-rabbit antibodies coupled to horseradish peroxidase (anti-mouse Tianjin Sungene Biotech Co., Ltd., LK2002; anti-rabbit Tianjin Sungene Biotech Co., Ltd., LK2001) were applied in 5% milk-TBST for 1 h at room temperature, and protein bands were revealed with chemiluminescence HRP substrate (Millipore, WBKLS0500). Protein loading volume and strip exposure time for every antibody were detected before the formal experiment. Band intensities were quantified using ImageJ software.

RNA isolation and RT-PCR analyses

Total RNA was extracted using TRIzol reagent (Invitrogen, 15,596–026) according to the manufacturer's instructions. cDNA was reverse transcribed from total RNA (DNase

treated) using M-MLV reverse transcriptase (Invitrogen, 28,025–013) and random hexamers (Invitrogen, 48,190–011).

Real-time-Pcr for Mir223 and Atg16l1 mRNA quantification

A SYBR Green Quantitative RT-PCR kit (Roche, 04–913,914-001) was used for single-step qRT-PCR reactions. To activate the SYBR green, an initial cycle of 95°C for 10 min was performed, followed by PCR reactions with 40 cycles of 95°C for 15 sec and 60°C for 1 min. Then, a thermal denaturation protocol was used to generate the dissociation curves to verify the amplification specificity (a single cycle of 95°C for 60 sec, 55°C for 60 sec and 80 cycles of 55°C for 10 sec). Changes in mRNA levels were quantified using the 2-ΔΔCT method with *Gapdh* (glyceraldehyde-3-phosphate dehydrogenase) mRNA as a control. The following primers were used: *Atg16l1* primers, 5'-CAGAGCAGCTACTAAGCGACT-3' and 5'-AAAAGGGGAGATTCGGACAGA-3'; *Gapdh* primers, 5'-AGCCACATCGCTCAGACAC-3' and 5'-GCCC AATACGACCAAATCC-3'; *Rnu6* primers, 5'-CTCGCTTC GGCAGCACA-3' and 5'-AACGCTTCACGAATTTGCGT; *Mir223* RT primers, 5'-GTCGTATCCAGTGCAGGGTCC GAGGTATTCGCACTGGATACGTGGGGTA-3' and *Mir223* primers, 5'-GCCCGfCCAGUUUGUCAAAUA-3' and 5'-GTGCAGGGTCCGAGGT-3'. Reactions were performed in duplicates and the number of independent experiments (n = 3) was indicated. The reactions were performed with a 7500 Fast Real-Time PCR System (Applied Biosystems, USA).

Statistical analyses

Statistical analyses were performed using Student's two-tailed t-test or ANOVA. Data were analyzed using Microsoft office Excel 2010 or SPSS Statistics 15 and presented as the mean ± SEM using the GraphPad Prism statistical program. Values of $p < 0.05$ were considered significant. No potential conflicts of interest were disclosed.

Disclosure statement

The authors have no financial conflict of interests.

Funding

This work was supported by the National Natural Science Foundation of China through No. 31600730, 81602496, 81501036, 81301026, 81302568, 81541032; Natural Science Foundation of Tianjin through Grant No. 16JCYBJC24800, 16JCYBJC24600; Science Foundation of Tianjin Medical University through Grant No.2012KYQ11; Postdoctoral Foundation of China through Grant 2016M591396.

References

[1] Lassmann H, van Horssen J, Mahad D. Progressive multiple sclerosis: pathology and pathogenesis. Nat Revi Neurol. 2012 Nov 5;8(11):647–656. PubMed PMID: 23007702.

[2] Martin R, Hernandez M, Cordova C, et al. Natural triterpenes modulate immune-inflammatory markers of experimental autoimmune encephalomyelitis: therapeutic implications for multiple sclerosis. Br J Pharmacol. 2012 Jul;166(5):1708–1723. PubMed PMID: 22260389; PubMed Central PMCID: PMC3419913.

[3] Goldmann T, Prinz M. Role of microglia in CNS autoimmunity. Clin Dev Immunol. 2013;2013:208093. PubMed PMID: 23840238; PubMed Central PMCID: PMC3694374.

[4] Ciccarelli O, Barkhof F, Bodini B, et al. Pathogenesis of multiple sclerosis: insights from molecular and metabolic imaging. Lancet Neurol. 2014 Aug;13(8):807–822. PubMed PMID: 25008549.

[5] Singh S, Metz I, Amor S, et al. Microglial nodules in early multiple sclerosis white matter are associated with degenerating axons. Acta Neuropathol. 2013 Apr;125(4):595–608. PubMed PMID: 23354834; PubMed Central PMCID: PMC3611040.

[6] Merson TD, Binder MD, Kilpatrick TJ. Role of cytokines as mediators and regulators of microglial activity in inflammatory demyelination of the CNS. Neuromolecular Med. 2010 Jun;12(2):99–132. PubMed PMID: 20411441.

[7] Liang P, Le W. Role of autophagy in the pathogenesis of multiple sclerosis. Neurosci Bull. 2015 Aug;31(4):435–444. PubMed PMID: 26254059.

[8] Zhen C, Feng X, Li Z, et al. Suppression of murine experimental autoimmune encephalomyelitis development by 1,25-dihydroxyvitamin D3 with autophagy modulation. J Neuroimmunol. 2015 Mar 15;280:1–7. PubMed PMID: 25773147.

[9] Feng X, Hou H, Zou Y, et al. Defective autophagy is associated with neuronal injury in a mouse model of multiple sclerosis. Bosnian J Med Sci. 2017 May 20;17(2):95–103. PubMed PMID: 28086065.

[10] Yan Q, Han C, Wang G, et al. Activation of AMPK/mTORC1-mediated autophagy by metformin reverses Clk1 deficiency-sensitized dopaminergic neuronal death. Mol Pharmacol. 2017 Dec;92(6):640–652. PubMed PMID: 29025968.

[11] Nash Y, Schmukler E, Trudler D, et al. DJ-1 deficiency impairs autophagy and reduces alpha-synuclein phagocytosis by microglia. J Neurochem. 2017 Dec;143(5):584–594. PubMed PMID: 28921554.

[12] Zhou X, Zhou J, Li X, et al. GSK-3beta inhibitors suppressed neuroinflammation in rat cortex by activating autophagy in ischemic brain injury. Biochem Biophys Res Commun. 2011 Jul 29;411(2):271–275. PubMed PMID: 21723251.

[13] Mizushima N. Autophagy: process and function. Genes Dev. 2007 Nov 15;21(22):2861–2873.

[14] Gozuacik D, Kimchi A. Autophagy as a cell death and tumor suppressor mechanism. Oncogene. 2004 Apr 12;23(16):2891–2906. PubMed PMID: 15077152.

[15] Ravikumar B, Sarkar S, Davies JE, et al. Regulation of mammalian autophagy in physiology and pathophysiology. Physiol Rev. 2010 Oct;90(4):1383–1435. PubMed PMID: 20959619.

[16] Martinez Vicente M, Cuervo AM. Autophagy and neurodegeneration: when the cleaning crew goes on strike. Lancet Neurol. 2007;6(4):352–361.

[17] Kimmelman AC. The dynamic nature of autophagy in cancer. Genes Dev. 2011 Oct 1;25(19):1999–2010.

[18] Mizushima N, Levine B. Autophagy in mammalian development and differentiation [10.1038/ncb0910-823]. Nat Cell Biol. 2010;12(9):823–830.

[19] Rubinsztein David C, Mariño G, Kroemer G. Autophagy and Aging. Cell. 2011;146(5):682–695.

[20] Lopez A, Lee SE, Wojta K, et al. A152T tau allele causes neurodegeneration that can be ameliorated in a zebrafish model by autophagy induction. Brain. 2017 Apr 01;140(4):1128–1146. PubMed PMID: 28334843; PubMed Central PMCID: PMC5382950.

[21] Wang P, Miao CY. Autophagy in the disorders of central nervous system: vital and/or fatal? CNS Neurosci Ther. 2012 Dec;18(12):955–956. PubMed PMID: 23191986.

[22] Abdel Fattah E, Bhattacharya A, Herron A, et al. Critical role for IL-18 in spontaneous lung inflammation caused by autophagy deficiency. J Immunol (Baltimore, Md 1950). 2015 Jun 01;194(11):5407–5416. PubMed PMID: 25888640; PubMed Central PMCID: PMC4433854.

[23] Wang Q, Zeng P, Liu Y, et al. Inhibition of autophagy ameliorates atherogenic inflammation by augmenting apigenin-induced macrophage apoptosis. Int Immunopharmacol. 2015 Jul;27(1):24–31. PubMed PMID: 25899084.
[24] Mehrpour M, Esclatine A, Beau I, et al. Overview of macroautophagy regulation in mammalian cells. Cell Res. 2010 Jul;20(7):748–762. PubMed PMID: 20548331.
[25] Mizushima N, Yoshimori T, Ohsumi Y. The role of Atg proteins in autophagosome formation. Annu Rev Cell Dev Biol. 2011;27:107–132. PubMed PMID: 21801009.
[26] Lemasters JJ. Selective mitochondrial autophagy, or mitophagy, as a targeted defense against oxidative stress, mitochondrial dysfunction, and aging. Rejuvenation Res. 2005 Spring;8(1): 3–5. PubMed PMID: 15798367.
[27] Kirisako T, Ichimura Y, Okada H, et al. The reversible modification regulates the membrane-binding state of Apg8/Aut7 essential for autophagy and the cytoplasm to vacuole targeting pathway. J Cell Biol. 2000 Oct 16;151(2):263–276. PubMed PMID: 11038174; PubMed Central PMCID: PMC2192639.
[28] Kabeya Y, Mizushima N, Ueno T, et al. LC3, a mammalian homologue of yeast Apg8p, is localized in autophagosome membranes after processing. Embo J. 2000 Nov 1;19(21):5720–5728. PubMed PMID: 11060023; PubMed Central PMCID: PMC305793.
[29] Tanida I, Ueno T, Kominami E. Human light chain 3/MAP1LC3B is cleaved at its carboxyl-terminal Met121 to expose Gly120 for lipidation and targeting to autophagosomal membranes. J Biol Chem. 2004 Nov 12;279(46):47704–47710. PubMed PMID: 15355958.
[30] Bjorkoy G, Lamark T, Brech A, et al. p62/SQSTM1 forms protein aggregates degraded by autophagy and has a protective effect on huntingtin-induced cell death. J Cell Biol. 2005 Nov 21;171 (4):603–614. PubMed PMID: 16286508; PubMed Central PMCID: PMC2171557.
[31] Klionsky DJ, Abdelmohsen K, Abe A, et al. Guidelines for the use and interpretation of assays for monitoring autophagy (3rd edition). Autophagy. 2016;12(1):1–222. PubMed PMID: 26799652; PubMed Central PMCID: PMC4835977.
[32] Fu LL, Wen X, Bao JK, et al. MicroRNA-modulated autophagic signaling networks in cancer. Int J Biochem Cell Biol. 2012 May;44(5):733–736. PubMed PMID: 22342941.
[33] Xu J, Wang Y, Tan X, et al. MicroRNAs in autophagy and their emerging roles in crosstalk with apoptosis. Autophagy. 2012 Jun;8 (6):873–882. PubMed PMID: 22441107; PubMed Central PMCID: PMC3427253.
[34] Wang Z, Yuan B, Fu F, et al. Hemoglobin enhances miRNA-144 expression and autophagic activation mediated inflammation of microglia via mTOR pathway. Sci Rep. 2017 Sep 19;7(1):11861. 10.1038/s41598-017-12067-2. PubMed PMID: 28928406; PubMed Central PMCID: PMC5605685.
[35] Jovicic A, Roshan R, Moisoi N, et al. Comprehensive expression analyses of neural cell-type-specific miRNAs identify new determinants of the specification and maintenance of neuronal phenotypes. J Neurosci. 2013;33(12):5127–5137.
[36] Sharaf-Eldin WE, Kishk NA, Gad YZ, et al. Extracellular miR-145, miR-223 and miR-326 expression signature allow for differential diagnosis of immune-mediated neuroinflammatory diseases. J Neurol Sci. 2017 Dec 15;383:188–198. PubMed PMID: 29246612.
[37] Cantoni C, Cignarella F, Ghezzi L, et al. Mir-223 regulates the number and function of myeloid-derived suppressor cells in multiple sclerosis and experimental autoimmune encephalomyelitis. Acta Neuropathol. 2017 Jan;133(1):61–77. 10.1007/s00401-016-1621-6. PubMed PMID: 27704281; PubMed Central PMCID: PMC5423756.
[38] Neely KM, Green KN. Presenilins mediate efficient proteolysis via the autophagosome-lysosome system. Autophagy. 2011 Jun;7(6):664–665. PubMed PMID: 21460614.
[39] Han HE, Kim TK, Son HJ, et al. Activation of autophagy pathway suppresses the expression of iNOS, IL6 and cell death of LPS-stimulated microglia cells. Biomol Ther (Seoul). 2013 Jan;21 (1):21–28. PubMed PMID: 24009854; PubMed Central PMCID: PMC3762303.
[40] Cheng M, Liu L, Lao Y, et al. MicroRNA-181a suppresses parkin-mediated mitophagy and sensitizes neuroblastoma cells to mitochondrial uncoupler-induced apoptosis. Oncotarget. 2016 Jul 5;7(27):42274–42287. PubMed PMID: 27281615; PubMed Central PMCID: PMC5173134.
[41] Xu F, Li J, Ni W, et al. Peroxisome proliferator-activated receptor-gamma agonist 15d-prostaglandin J2 mediates neuronal autophagy after cerebral ischemia-reperfusion injury. PloS one. 2013;8(1): e55080. PubMed PMID: 23372817; PubMed Central PMCID: PMC3555818.
[42] Lu C, Chen J, Xu HG, et al. MIR106B and MIR93 prevent removal of bacteria from epithelial cells by disrupting ATG16L1-mediated autophagy. Gastroenterology. 2014 Jan;146(1):188–199. PubMed PMID: 24036151; PubMed Central PMCID: PMC3870037.
[43] Zhai Z, Wu F, Dong F, et al. Human autophagy gene ATG16L1 is post-transcriptionally regulated by MIR142-3p. Autophagy. 2014 Mar;10(3):468–479. PubMed PMID: 24401604; PubMed Central PMCID: PMC4077885.
[44] Wang IK, Sun KT, Tsai TH, et al. MiR-20a-5p mediates hypoxia-induced autophagy by targeting ATG16L1 in ischemic kidney injury. Life Sci. 2015 Sep 1;136:133–141. PubMed PMID: 26165754.
[45] Sun KT, Chen MY, Tu MG, et al. MicroRNA-20a regulates autophagy related protein-ATG16L1 in hypoxia-induced osteoclast differentiation. Bone. 2015 Apr;73:145–153. PubMed PMID: 25485521.
[46] Guo L, Zhao J, Qu Y, et al. microRNA-20a inhibits autophagic process by targeting ATG7 and ATG16L1 and favors mycobacterial survival in macrophage cells. Front Cell Infect Microbiol. 2016;6:134. PubMed PMID: 27803889; PubMed Central PMCID: PMC5067373.
[47] Mizushima N, Komatsu M. Autophagy: renovation of cells and tissues. Cell. 2011 Nov 11;147(4):728–741. PubMed PMID: 22078875.
[48] Kuballa P, Nolte WM, Castoreno AB, et al. Autophagy and the immune system. Annu Rev Immunol. 2012;30:611–646. PubMed PMID: 22449030.
[49] Masiero E, Sandri M. Autophagy inhibition induces atrophy and myopathy in adult skeletal muscles. Autophagy. 2010 Feb;6(2):307–309. PubMed PMID: 20104028.
[50] Korkmaz G, le Sage C, Tekirdag KA, et al. miR-376b controls starvation and mTOR inhibition-related autophagy by targeting ATG4C and BECN1. Autophagy. 2012 Feb 1;8(2):165–176. PubMed PMID: 22248718.
[51] Dorhoi A, Iannaccone M, Farinacci M, et al. MicroRNA-223 controls susceptibility to tuberculosis by regulating lung neutrophil recruitment. J Clin Invest. 2013 Nov 1;123(11):4836–4848. PubMed PMID: 24084739.
[52] Xi X, Zhang C, Han W, et al. MicroRNA-223 is upregulated in active tuberculosis patients and inhibits apoptosis of macrophages by targeting FOXO3. Genet Test Mol Biomarkers. 2015 Dec;19(12):650–656. PubMed PMID: 26505221.
[53] Shao BZ, Wei W, Ke P, et al. Activating cannabinoid receptor 2 alleviates pathogenesis of experimental autoimmune encephalomyelitis via activation of autophagy and inhibiting NLRP3 inflammasome. CNS Neurosci Ther. 2014 Dec;20(12):1021–1028. PubMed PMID: 25417929.
[54] Weindel CG, Richey LJ, Bolland S, et al. B cell autophagy mediates TLR7-dependent autoimmunity and inflammation. Autophagy. 2015;11(7):1010–1024. PubMed PMID: 26120731; PubMed Central PMCID: PMC4590645.
[55] van Loosdregt J, Rossetti M, Spreafico R, et al. Increased autophagy in CD4+ T cells of rheumatoid arthritis patients results in T-cell hyperactivation and apoptosis resistance. Eur J Immunol. 2016 Oct 5 PubMed PMID: 27624289. DOI:10.1002/eji.201646375
[56] Stromnes IM, Goverman JM. Active induction of experimental allergic encephalomyelitis. Nat Protoc. 2006;1(4):1810–1819. PubMed PMID: 17487163.